MedChemComm

Cite this: *Med. Chem. Commun.*, 2012, **3**, 710

www.rsc.org/medchemcomm

CONCISE ARTICLE

Optimization of a series of dipeptides with a P3 β-neopentyl asparagine residue as non-covalent inhibitors of the chymotrypsin-like activity of human 20S proteasome†

Christopher Blackburn,* Cynthia Barrett, Jonathan L. Blank, Frank J. Bruzzese, Nancy Bump, Lawrence R. Dick, Paul Fleming, Khristofer Garcia, Paul Hales, Matthew Jones, Jane X. Liu, Masayuki Nagayoshi, Darshan S. Sappal, Michael D. Sintchak, Christopher Tsu, Cindy Xia, Xiansi Zhou and Kenneth M. Gigstad

Received 29th February 2012, Accepted 16th April 2012
DOI: 10.1039/c2md20060k

Inhibition of the proteasome by covalent inhibitors is a clinically proven anti-cancer therapy. We report here that dipeptides with a P3 neopentyl Asn residue are potent, reversible, non-covalent inhibitors selective for the chymotryptic activity of the 20S proteasome *in vitro* and in cells. The X-ray structure of compound **20** in complex with yeast 20S reveals the importance of hydrophobic bonding interactions of the neopentyl group within the S3 binding pocket of the 20S β5 sub-unit. Four compounds show comparable potencies to boronic acid inhibitors in a panel of assays.

1. Introduction

The ubiquitin-proteasome pathway is responsible for the regulated degradation of intracellular proteins, including those involved in signal transduction, cell cycle control, apoptosis and inflammation.[1–3] Inhibition of the 20S core particle of the proteasome causes accumulation of substrate proteins leading to apoptosis and is preferentially cytotoxic to cancer cells.[4,5] The active sites of 20S located on the β1, β2, and β5 subunits (classified as caspase-like, trypsin-like, and chymotrypsin-like, respectively) catalyze proteolysis of substrates by nucleophilic attack of the hydroxyl group of the *N*-terminal threonine residues (Thr1O$^{\gamma}$) on peptide bonds.[6,7] Numerous 20S inhibitors have been described[8] that form covalent adducts with the active site threonine hydroxyls including peptidic aldehydes, vinyl sulfones,[3] vinylacylpyrroles,[9] α,β-epoxyketones[10,11] such as carfilzomib (Fig. 1), 2-keto-1,3,4-oxadiazoles,[12] β-lactones[13–15] *e.g.* salinosporamide A, β-lactams[16] and boronic acids.[17–21] The dipeptide boronic acid bortezomib is used clinically to treat multiple myeloma and relapsed mantle cell lymphoma, and is being evaluated for the treatment of other malignancies.[22] Bortezomib forms a slowly reversible adduct with the *N*-terminal threonine of the 20S β5 site (K_i = 0.55 nM; dissociation $t_{1/2}$ *ca.* 110 min)[7,8] which has been characterized by X-ray crystallography.[18] Two additional boronic acids MLN9708[8,19] and CEP-18770[20,21] are undergoing clinical trials.

Non-covalent inhibitors of the catalytic β sub-units of the 20S core particle are less well described even though they may show more widespread tissue distribution than their covalent counterparts due to rapid dissociation from the 20S sub-unit in the blood compartment. Among the non-covalent inhibitors reported, cyclic peptide TMC-95A, competitively inhibits the chymotrypsin-like activity of the proteasome with nanomolar potency[23] although synthetic analogs show only moderate potency.[24] Several dipeptide inhibitors[25–32] have been described (Fig. 2), notably trimethoxy-L-phenylalanine derivative (**1**) which has been shown to inhibit the β5 activity reversibly.[26–29] Recently, we described the biological properties of screening hit **2**,[32] a rapid-equilibrium inhibitor of the β5 (chymotrypsin-like) activity of the proteasome that does not inhibit the activity of the β1 or β2 sites. Compound **2** also inhibits TNFα-induced activation of NFκB-Luc in HEK293 cells consistent with proteasome inhibition and is cytotoxic toward human cancer cell lines. We therefore investigated dipeptide analogs of **2** preparing over 1500 derivatives using automated solution-phase synthesis[33] and reported the detailed biological properties of fifteen compounds representative of several sub-series[32] followed by a description of the SAR of the P3 Thr series including potent non-covalent inhibitors such as **3** and **4**.[34] Crystal structures of several inhibitors in complex with yeast 20S demonstrated the non-covalent binding interactions with the β5 sub-unit and suggested that replacement of the P3 Thr by a bulky hydrophobic residue might lead to a more optimal occupancy of the S3 binding pocket. Of several residues investigated at this position,[35] the β-neopentyl asparagine group, previously incorporated only in covalent

Discovery, Millennium Pharmaceuticals, Inc., 40 Landsdowne Street, Cambridge, MA 02139, USA. E-mail: blackburn@mpi.com; Tel: +1 617 761 6811

† Electronic supplementary information (ESI) available: Crystallographic data and refinement statistics. See DOI: 10.1039/c2md20060k

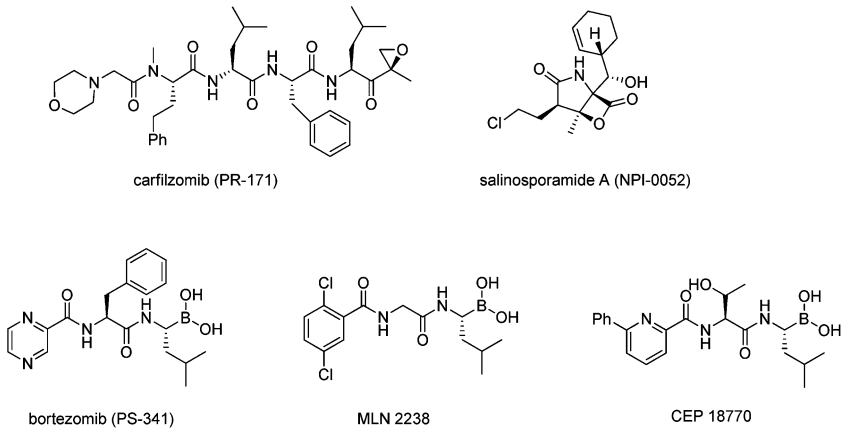

Fig. 1 Covalent proteasome inhibitors.

inhibitors[12] leads to potent, selective and reversible inhibition of the β5 sub-unit of 20S as discussed in this paper.

2. Chemistry

Initially, we approached the further optimization of dipeptides by retaining the P1 benzylic and P2 homoPhe residues previously shown to contribute to the potency of compounds such as **3** and **4** while replacing the P3 Thr with larger residues. The key amino acid amides **5** were prepared as shown in Scheme 1. Coupling of **5a** with an orthogonally protected diaminopropanoic acid followed by removal of the side-chain CBZ protecting group gave **6b** which was treated with dimethylbutanoic acid to install the branched P3 residue. Deprotection of the terminal amino group followed by *N*-terminal capping with three aryl carboxylic acids afforded analogs **9–11**.

The key intermediate towards P3 neopentyl asparagine derivatives, *N*-α-Boc-β-neopentyl asparagine **8** was prepared as described previously[32] and incorporated into peptides by solution phase parallel synthesis as shown in Scheme 2.

Analogs **34** and **35** in which the neopentyl amide side-chain was replaced by smaller alkyl groups and heterocyclic replacements for the neopentyl amide side-chain (oxadiazoles **36** and **37**) were also investigated (Scheme 3). Thus, the side-chain protected aspartic acid derivative **38** was prepared, subjected to hydrogenolysis, and the resulting acid **39** coupled to *tert*-butylhydroxyamidine and cyclized[36] by microwave irradiation in pyridine solution to give **40** which was further elaborated to compounds **36** and **37**. Coupling the side-chain acid of **39** to *n*-propylamine or isobutylamine, deprotection of the *N*-terminal amino group and aroylation afforded **34** and **35**, respectively.

3. Results and discussion

The inhibitory activities of compounds **9–37** on the rate of hydrolysis of the β5 substrate Ac-WLA-AMC catalyzed by human 20S constitutive proteasome were determined and selectivity assessed by measuring inhibition of the hydrolysis of β1 (Z-LLE-AMC) and β2 (Ac-KQL-AMC) selective substrates.[32] Potencies were also determined in the Proteasome-Glo™ cell-based assay that measures directly the peptidase activity of the β5 site of the 26S proteasome in cells using a luminogenic chymotrypsin-like substrate. We also assessed the effects of the compounds on activation of the transcription factor NFκB[30,37] in cells in conjunction with cell viability experiments in which cellular ATP levels were determined by ATPlite assay in the human lung cancer cell line Calu6 (Table 1). In our earlier work on related dipeptides[32–35] we found that compounds with relatively small P3 residues exhibit little 20S inhibition unless a compensating large aryl-containing P4 residue is present. For

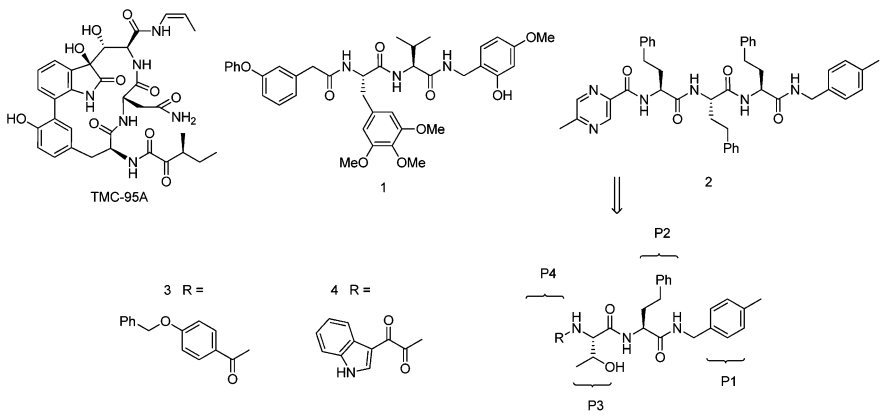

Fig. 2 Non-covalent proteasome inhibitors.

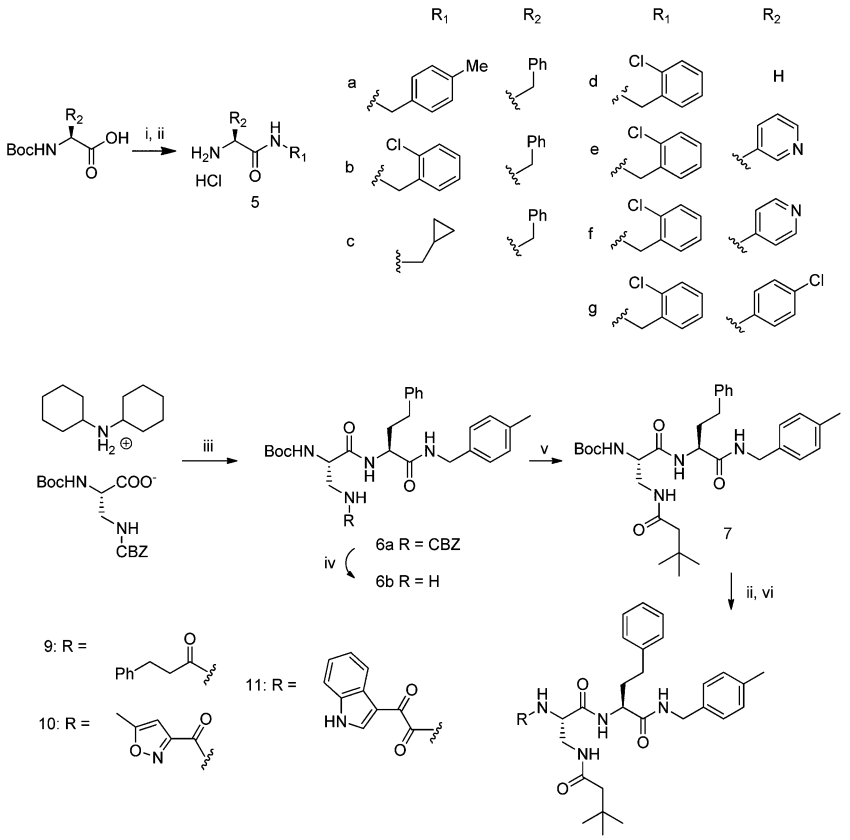

Scheme 1 Synthesis of P3-diaminopropanoic acid peptides. *Reagents and conditions*: (i) R_1NH_2, HBTU, NMM, DCM; (ii) 4 M HCl in dioxane; (iii) **5a**, HATU, NMM, DCM, 25 °C, 16 h; (iv) H_2 (1 atm), 10% Pd–C, i-PrOH, 4 h; (v) Me_3CH_2COOH, HATU, NMM, DCM, 25 °C, 16 h; (vi) RCOOH, HBTU, NMM, DCM.

example, while compounds **3** and **4** possess respectable potencies, analogous compounds with simple acyl groups at the P4 position invariably show IC_{50} values >1 μM. In contrast, all the P3 neopentyl Asn derivatives, including analogs **12** and **13** with small P4 residues, show relatively high β5 inhibitory potencies without any effect on β1 or β2 activity (Table 1). When the P4 residue was extended with alicyclic (compound **14**) or aryl residues (analogs **15–20**) significant improvements in inhibitory activity were observed. In general, we observed a good correlation between the inhibition of 20S β5 activity *in vitro* and proteasome inhibition in cells as measured by the Proteasome-Glo and NFκB-Luc assays. Derivatives **18** and **19** are considerably more potent inhibitors than their P3 Thr counterparts (compounds **3** and **4** respectively) in all four assays, particularly in cells. The reverse amide analogs, namely diaminopropionic acid derivatives **9–11**, proved to be considerably less active and this series was not pursued further. Interestingly, while the large hydrophobic P4 residues improved potency of the neopentyl Asn series, they were not essential as demonstrated by the inhibitory activities of isoxazole derivative **20**. Reduced inhibitory activity resulted from replacement of the P1 benzylic group by the smaller cyclopropylmethyl (compare compounds **16** and **21**). The importance of the branched P3 side-chain for enzyme inhibition was demonstrated by the considerably lower activity of the *n*-propyl compound **34** while the iso-butyl derivative **35** had comparable enzyme inhibitory activity to neopentyl analog **20**. Attempts to find potent heterocyclic replacements for the neopentyl Asn side-chain were largely unsuccessful[35] with the exception of the *tert*-butyl-1,2,4-oxadiazole isostere. Even here, compounds **36** and **37** showed significant reductions in activity in comparison with their neopentyl Asn analogs **19** and **20**.

A co-crystal of compound **20**, in complex with yeast open gate 20S is depicted in Fig. 3. We observed the same general non-covalent binding mode that we reported earlier for compound

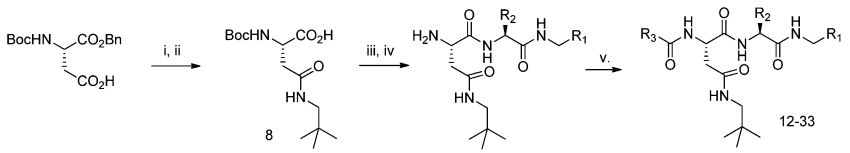

Scheme 2 Synthesis of P3-neopentyl asparagine peptides. *Reagents and conditions*: (i) neopentylamine, HOBt, NMM, DCM, 25 °C, 24 h; (ii) H_2 (1 atm), 10% Pd/C, MeOH, 25 °C, 3 h; (iii) **5a–g**, HBTU, NMM, DMF, 25 °C, 24 h; (iv) 4 N HCl, dioxane, 2 h; (v) RCOOH, HBTU, NMM, DMF, 25 °C, 24 h.

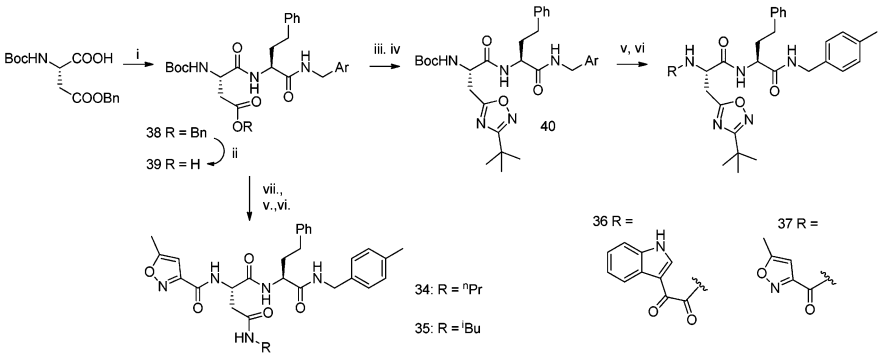

Scheme 3 Synthesis of P3 asparagine and oxadiazole-containing peptides. *Reagents and conditions*: (i) **5a**, HBTU, NMM, DMF, 25 °C, 16 h. (ii) H_2, 10% Pd–C, MeOH, 1 atm; (iii) *t*-Bu(NH_2)C=NOH, EDC, DCM, DMF, 25 °C, 24 h; (iv) pyridine, 110 °C, MWI, 20 min; (v) 4 N HCl, dioxane, 2 h; (vi) RCOOH, HBTU, NMM, DMF; (vii) RNH_2, HBTU, NMM, DMF.

29[32–34] including backbone H-bonding interactions with several residues of the β5 sub-unit, *viz.* Gly47, Thr21 and (*via* a bridging water molecule) Ala49 and Ala50. There is also evidence for an interaction between the carbonyl oxygen of the neopentyl Asn side-chain and Ser118 of the β6 sub-unit (Fig. 3a). The P1 benzyl group occupies a well-defined S1 binding pocket with an additional hydrophobic interaction taking place between the 4′-methyl group and a sub-pocket of S1. Although P2 residues point out toward solvent, the two methylene groups of homoPhe permit a conformation in which the π-system of the aryl group forms a ledge interaction with Gly47-Gly48. The very large S4 pocket can be partially occupied by a range of *N*-terminal residues that likely contribute to potency by picking up further hydrophobic interactions. We attribute the generally high potencies of compounds in this series to the near optimal fit of the neopentyl-Asn P3 substituent in the S3 binding pocket of the β5 sub-unit (Fig. 3b). A crystal structure of yeast 20S in complex with *tert*-butyloxadiazole **37** was also obtained and the binding mode is compared with that of P3 neopentyl Asn analog **20** in Fig. 4. While the backbone conformations of these compounds in the bound mode are very similar, the pendant *tert*-butyl group of **37** displaces His98 of the β6 sub-unit rather than projecting optimally into the β5 S3 binding pocket accounting for the loss in inhibitory activity.

We next investigated analogs with an 2′-chlorobenzyl residue in the P1 position reasoning that the interaction of chlorine with a S1 sub-pocket observed in earlier series[32,34] would contribute to affinity and that these derivatives would be less susceptible to oxidative metabolism than the 4′-methyl counterpart. (Incubation of compound **18**, for example, with human or rodent liver microsomes followed by LC-MS-MS analysis indicated that ring hydroxylation of the P1 and P2 residues contributes to low

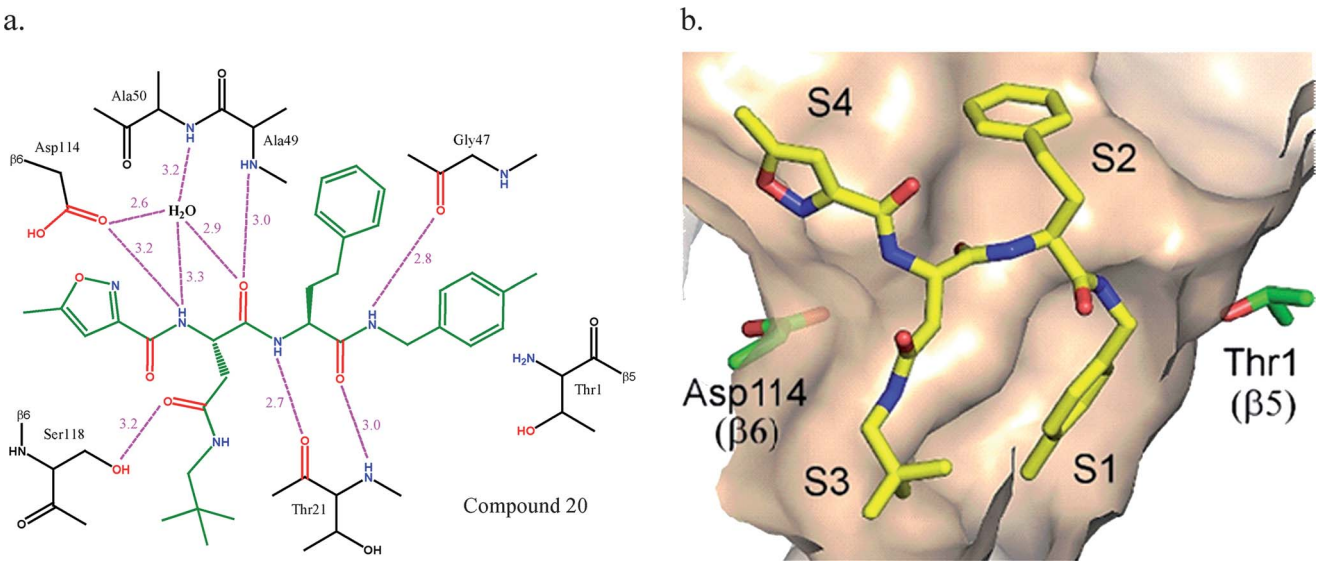

Fig. 3 (a) Schematic representation of the β5/β6 active site of 20S with compound **20** bound. Key hydrogen bonds between the inhibitor and the protein are shown as dashed lines colored magenta, with distances indicated in Angstroms. (b) Molecular surface of 20S with compound **20** bound, showing specificity pockets S1–S4. Atoms are shown in ball and stick representation with carbon in yellow, nitrogen in blue and oxygen in red. The side chain atoms for Thr2 (β5) and Asp114 (β6) are shown with carbon colored green. Figure made using PyMOL Molecular Graphics System (DeLano Scientific, Palo Alto, CA).

Table 1 Enzymatic, cellular and anti-proliferative effects of P3 neopentyl Asn and Thr dipeptides compared with boronates

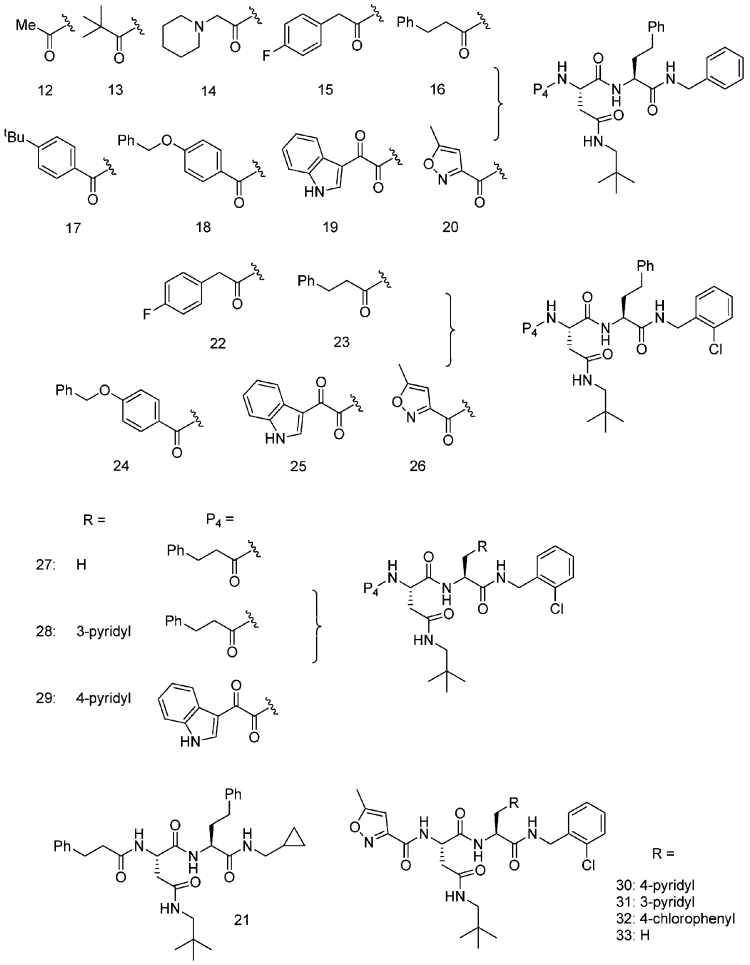

Compound	Human 20S β5c IC_{50} (nM)[a]	Calu6 β5c IC_{50} (nM)[b]	NFκB-Luc IC_{50} (nM)[c]	Calu6 LC_{50} (nM)[d]	Compound	Human 20S β5c IC_{50} (nM)[a]	Calu6 β5c IC_{50} (nM)[b]	NFκB-Luc IC_{50} (nM)[c]	Calu6 LC_{50} (nM)[d]
Bortezomib[8]	2.0	3.9	9.7 (100)	5.2	**21**	12	360	38 (86)	150
MLN223[8]	3.0	9.0	6.2 (100)	14[d]	**22**	4.0	85	110 (80)	94
2[32]	16.0	53.0	45 (79)	130	**23**	3.0	18	18 (86)	20
3[34]	20.0	159	120 (81)	280	**24**	11	12	39 (90)	4.7
4[34]	7.3	14	90 (100)	200	**25**	3.7	11	17 (98)	2.4
9	>1000	ND	ND	ND	**26**	2.1	13	9 (85)	41
10	>1000	ND	ND	ND	**27**[32]	4.0	35	10 (74)	39
11	910	ND	ND	ND	**28**[32]	3.9	24	9 (77)	61
12	50	960	150 (80)	890	**29**[32]	1.2	9.5	12.0 (92)	6
13	25	610	62 (90)	210	**30**	33.3	940	950 (85)	210
14	12	30	62 (85)	180	**31**	22.6	690	140 (80)	170
15	8.4	73	23 (79)	120	**32**	16.0	ND	320 (93)	1100
16	5.4	17	12 (80)	89	**33**	23.0	1400	120 (80)	200
17	22	40	32 (86)	31	**34**	160	ND	ND	ND
18[32]	6.8	11	22 (78)	10.0	**35**	7.3	ND	53 (88)	250
19	4.8	9.7	25 (97)	2.6	**36**	11.6	30	110 (98)	36
20	4.7	25	9 (85)	27	**37**	93	1700	900 (82)	1500

[a] Human erythrocyte 20S was used as a source of constitutive proteasome. All compounds showed negligible inhibition (IC_{50} values >10 000 nM) of the cleavage of β1 (Z-LLE-AMC) and β2 (Ac-KQL-AMC) substrates. Data are means of at least three independent measurements. [b] Cell-based (Proteasome-Glo) assay measuring peptidase activity of the β5 site of the 26S proteasome. [c] Inhibition of NFκB-luciferase activity in HEK293 cells stimulated with TNF-α; % maximal inhibition values are shown in parentheses.[32] [d] Anti-proliferative effects in Calu6 ATPlite (Perkin Elmer) cell viability assay. Data for compound **4** acquired with H460 cells. ND not determined.

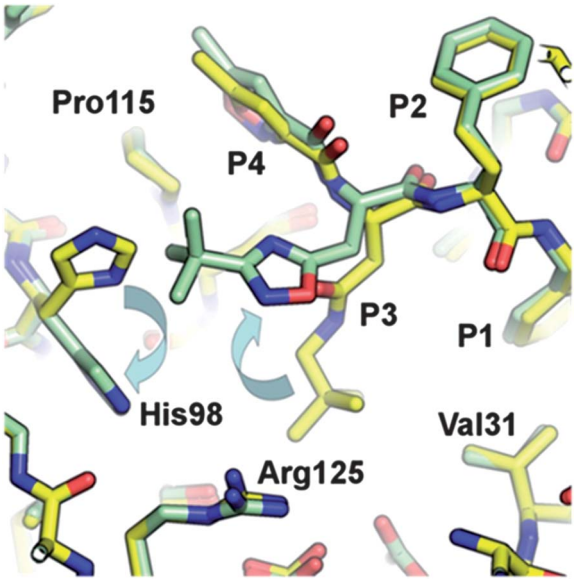

Fig. 4 Superposition of the structures for compounds **20** and **37** bound to the β5/β6 active site of 20S, highlighting the S3 pocket and changes in the position of His98. All residues labeled are from the β6 sub-unit, with the exception of Val31 (β5). Coloring scheme is as described above, with carbon atoms for **20** shown in yellow and **37** in green.

metabolic stability (extraction ratio $E_h > 0.9$) of this and related compounds.) In general, the same trends in inhibitory activity as a function of P4 residue were observed as with the previous series. Thus, with homoPhe as the P2 residue, the pairs of compounds **15** and **22**; **16** and **23**; **18** and **24**; **19** and **25**; **20** and **26** showed comparable potencies in each of the four assays. We also investigated P2 residues with a lower potential for oxidative metabolism by replacing homoPhe by Ala or by electron deficient pyridyl residues. In the case of P4 phenylpropionyl derivatives **27** and **28** loss of the ledge interaction present with **23** had little effect on enzymatic or cellular potency whereas in the isoxazole series analogs **30**, **31**, **32** and **33** were less potent than the homoPhe analog **26**. In contrast, P2 4-pyridylalanine derivative **29** was found to have comparable potencies to homoPhe analog **25**. Indeed, compounds **25** and **29** showed the best combination of enzymatic and cellular activities of all the compounds prepared to date including anti-proliferative effects comparable to those of the boronates. The reason that P4 ketoindole residues confer high potencies is unclear though we have shown previously[32] that there is no evidence of any covalent interactions with 20S and thus the group presumably acts as a constrained version of the phenylpropionyl residue. As well as demonstrating selective inhibition of the chymotryptic activity of the proteasome, this series of compounds is selective for unrelated proteases. For example, compounds **25** and **26** did not show any significant inhibitory activity on a panel of purified human proteases including cathepsin B and L, coagulation factor b-XIIa, chymotrypsin, elastase, plasmin, thrombin, tissue plasminogen activator, trypsin and calpain I at concentrations of 100 μM. Unfortunately, although compounds such as **29** designed to be metabolically more stable afforded fewer metabolites in microsomal stability experiments extraction ratios remained very high due to oxidative metabolism of the neopentyl group.

4. Conclusions

In summary, we have found that dipeptides with a P3 neopentyl Asn residue are reversible non-covalent inhibitors of the β5 sub-unit of 20S with unprecedented potency and selectivity over the human β1 and β2 sub-units (IC_{50} > 10 μM) attributable to the near optimal fit of this substituent in the S3 binding pocket of the 20S β5 sub-unit. In general, we observed a good correlation between the inhibitory IC_{50} values for 20S β5 activity *in vitro* and proteasome inhibition in cells as measured by the Proteasome-Glo™ assay and by NFκB-Luc activity with several derivatives showing improved cellular activities compared to tripeptide **8** and some of the compounds (for example, **18**, **19**, **25** and **29**) having comparable potencies to the boronates. The cytotoxic LC_{50} values of these compounds in Calu6 cells also correlate with their 20S β5 potencies and support the premise that selective non-covalent inhibition of the β5 (chymotrypsin-like) site of the proteasome is sufficient to inhibit TNFα-dependent NFκB activity and the proliferation of cancer cells.

5. Experimental

Compound synthesis and characterization

General. NMR spectra were recorded on a Bruker 300 MHz Avance1 or 400 MHz Avance2 (5 mm QnProbe) using residual solvent peaks as the reference. Compound purity was determined by analysis of the diode array UV trace of an LC-MS spectrum using the following procedure. Compounds were dissolved in DMSO, methanol or acetonitrile and the solutions were analyzed using an Agilent 1100 LC interfaced to a micromass Waters® Micromass® Zspray™ Mass Detector (ZMD). One of two gradients was used to elute the compounds either a formic acid (FA) gradient (acetonitrile containing 0 to 100 percent 0.1% formic acid in water) or an ammonium acetate (AA) gradient (acetonitrile containing zero to 100 percent 10 mM ammonium acetate in water). All compounds were determined to be >95% pure. High-resolution mass spectra were recorded using a QSTAR® XL quadrupole time-of-flight mass spectrometer (Applied Biosystems) coupled to an 1100 series HPLC system (Agilent Technologies). An isocratic flow of 40% H_2O 60% MeCN containing 0.1% HOAc at 200 μL min^{-1} was used to deliver each sample to the electrospray source tuned in ESI TOF-MS positive mode with a 3 min acquisition time for each analysis. The mass spectrometer was externally calibrated between *m/z* 400–800 by using API Calibration (NaCsI) Solution. For each analysis, approximately 5 scans were summed and the centroid *m/z* value of the protonated monoisotopic molecular ion $[M + H]^+$ was recorded. For each compound, the experimental and calculated [M + H] values were within ±4 ppm, supporting their expected elemental composition.

General synthetic procedures

(*S*)-2-(*tert*-Butoxycarbonylamino)-4-(neopentylamino)-4-oxobutanoic acid (**8**) and *C*-terminal capped amino acids (**5**) were prepared as described previously.[32]

*(S)-2-Amino-N-(4-methylbenzyl)-4-phenylbutanamide hydrochloride (**5a**)*: mp 109–112 °C. Found C, 67.28%; H, 6.74%; N, 8.65%: calcd for $C_{18}H_{23}ClN_2O$ C, 67.81%; H, 7.27%; N, 8.79%.

*(S)-2-Amino-N-(2-chlorobenzyl)-4-phenylbutanamide hydrochloride (**5b**)*: mp 166–167 °C. Found C, 60.14%; H, 5.80%; N, 8.24%: calcd for $C_{17}H_{20}Cl_2N_2O$; C, 60.18%; H, 5.94%; N, 8.26%.

Preparation of benzyl *tert*-butyl ((*S*)-3-(((*S*)-1-((4-methylbenzyl) amino)-1-oxo-4-phenylbutan-2-yl)amino)-3-oxopropane-1,2-diyl)dicarbamate (6a)

A solution of the dicyclohexylamine salt of *N*-α-Boc-CBZ-diaminopropionic acid (1.0 g, 1.9 mmol) in DMF (7 mL) and dichloromethane (3 mL) was treated with **5a** hydrochloride (0.58 g, 1.83 mmol), HATU (0.695 g, 1.83 mmol), *N*-methylmorpholine (0.6 mL, 5.5 mmol) and stirred at ambient temperature for 16 h. The DCM was evaporated under reduced pressure and the residual solution poured onto ice cold saturated $NaHCO_3$ solution and the precipitate collected and recrystallized from ethyl acetate to give **6a** (0.65 g, 60%) ^{1}HMR (400 MHz, d_6-DMSO) δ: 8.30 (m, 1H), 8.10 (m, 1H), 7.37–7.06 (m, 15H), 6.95 (m, 1H), 4.95 (m, 2H), 4.24 (m, 2H), 4.09 (m, 1H), 2.55 (m, 2H), 2.25 (s, 3H), 1.98 (m, 1H), 1.85 (m, 1H), 1.38 (s, 9H).

Preparation of compounds 9–11

Compound **6a** (181 mg, 0.3 mmol) was dissolved in isopropanol (50 mL), with heating, treated with 10% Pd/carbon and hydrogenated at balloon pressure for 16 h. The catalyst was removed and the solvent evaporated under reduced pressure to give **6b** LC-MS [M + H] 470 which was redissolved in DMF (3.0 mL) and treated with *tert*-butylacetic acid (42 μL, 0.33 mmol), HATU (125 mg, 0.33 mmol) and diisopropylethylamine (108 μL, 0.66 mmol) and stirred at ambient temperature for 16 h. The reaction mixture was diluted with ice cold saturated aqueous sodium bicarbonate solution and the resulting precipitate collected. The crude product was purified by reverse phase chromatography on a C-18 column eluting with water–MeCN gradient (0.1% formic acid) and the desired fractions lyophilized to give **7** (144 mg, 85%). ^{1}H NMR (400 MHz, d_4-MeOH) δ: 7.3–7.10 (m, 9H), 4.40–4.30 (m, 2H), 4.20 (m, 1H), 3.50–3.45 (m, 2H), 3.34–3.31 (m, 4H), 2.74–2.60 (m, 1H), 2.31 (s, 2H), 2.15–1.94 (m, 4H), 1.44 (s, 9H), 1.01 (s, 9H).

A solution of **7** (31 mg, 0.056 mmol) in dioxane (1.0 mL) was treated with 4 M HCl in dioxane (1.0 mL) and stirred at ambient temperature for 2 h whereupon LC-MS analysis ([M + H] 467) indicated that deprotection was complete. The reaction mixture was evaporated under reduced pressure and the residue suspended in dichloromethane (3 mL) and treated with *N*-methylmorpholine (18 μL, 0.157 mmol), 5-methylisoxazole-3-carboxylic acid (7.8 mg, 0.061 mmol) and a solution of HBTU (23 mg, 0.061 mmol) in DMF (0.5 mL). After stirring for 16 h at ambient temperature, the dichloromethane was evaporated and the residue diluted with ice cold saturated aqueous sodium bicarbonate solution and the resulting precipitate collected. The crude product was purified by reverse phase chromatography on a C-18 column eluting with water–MeCN gradient (0.1% formic acid) and the desired fractions lyophilized to give **10** (27 mg, 87%). LC-MS [M + H] 576. ^{1}H NMR (400 MHz, d_4-MeOH) 7.3–7.0 (m, 9H), 6.34 (s, 1H), 4.56 (t, 1H), 4.27 (m, 1H), 4.25 (s, 2H), 3.58 (m, 2H), 2.56 (m, 2H), 2.38 (s, 3H), 2.20 (s, 3H), 2.10–1.82 (m, 4H), 0.86 (s, 9H).

Compounds **9** and **11** were prepared similarly.

9: ^{1}HMR (400 MHz, CD_3OD) δ: 1.05 (s, 9H), 1.98 (m, 1H), 2.13 (s, 2H), 2.29 (s, 3H), 2.47 (t, J = 8 Hz, 2H), 2.66 (m, 2H), 2.87 (t, J = 8 Hz, 2H), 3.44 (m, 1H), 3.62 (m, 1H), 4.36 (m, 2H), 4.49 (t, 1H, J = 8 Hz), 7.10–7.28 (m, 9H).

11: ^{1}HMR (400 MHz, d_8-THF) δ: 9.00 (s, 1H), 8.39 (m, 1H), 7.43 (m, 1H), 7.23–7.04 (m, 11H), 4.51–4.25 (m, 4H), 3.91 (m, 1H), 3.53 (m, 1H), 2.64 (m, 1H), 2.00 (m, 4H), 1.85 (m, 2H), 1.00 (s, 9H).

Synthesis of capped peptides 9–35

Compounds were prepared using the solution phase parallel amide synthesis techniques described previously.[32,34] Amide couplings were effected using HBTU and *N*-methylmorpholine (NMM) in DMF solution. After evaporation of the solvent in a Genevac HT-12, crude products were dissolved in $CHCl_3$: THF (3 : 1) and extracted with saturated aqueous $NaHCO_3$. All final compounds were purified by preparative reverse phase HPLC using mass-directed fraction collection conducted on an Agilent 1100 series LC/MSD instrument using a Waters SunFire C-18 5 μm preparative OBD column (19 × 150 mm). The compounds were eluted with a water–MeCN gradient (0.1% formic acid) optimized by the A2Prep Agilent software. Final products described in the manuscript were further characterized by ^{1}H NMR spectroscopy and high resolution mass spectrometry.

32: ^{1}HMR (400 MHz, CD_3OD) δ: 0.83 (s, 9H), 2.51 (s, 3H), 2.73 (dd, J = 12 Hz, J = 7 Hz, 1H), 2.86 (dd, J = 12 Hz, J = 7 Hz, 1H), 2.90 (s, 2H), 2.95 (dd, J = 12 Hz, J = 7 Hz, 1H), 3.22 (dd, J = 12 Hz, J = 7 Hz, 1H), 4.48 (m, 2H), 4.66 (m, 1H), 6.46 (s, 1H), 7.15–7.25 (m, 7H), 7.39 (m, 1H).

In some cases compounds prepared by parallel synthesis as described above were scaled-up using conventional techniques as described below.

(*S*)-*N*1-((*S*)-1-(4-Methylbenzylamino)-1-oxo-4-phenylbutan-2-yl)-2-(5-methylisoxazole-3-carboxamido)-*N*4-neopentylsuccinamide (20)

A suspension of 5-methylisoxazole-3-carboxylic acid (0.017 g, 0.13 mmol) in anhydrous dichloromethane (1.0 mL) was treated with DMF (1.8 μL, 0.024 mmol) followed by oxalyl chloride (12 μL, 0.14 mmol) and stirred at ambient temperature for 1.5 h. Volatiles were removed under vacuo and the residue re-dissolved in dichloromethane (1 mL) and added to a solution of (2*R*)-2-amino-*N*∼4∼-(2,2-dimethylpropyl)-*N*∼1∼-{(2*R*)-1-[(4-methylbenzyl)amino]-1-oxo-4-phenylbutan-2-yl}succinamide (0.06 g, 0.1 mmol) in dichloromethane (1.0 mL). *N*-Methylmorpholine (0.1 mL, 0.9 mmol) was next added and the mixture was stirred at ambient temperature for 4 h. The resulting suspension was diluted with dichloromethane–hexane 1 : 1 (3 mL) and the precipitate collected. The crude product was dissolved in DCM–MeOH applied to silica gel thick layer plates and eluted with 20% ethyl acetate in dichloromethane. Extraction of the main band afforded **20** (48 mg, 83%). ^{1}H NMR (400 MHz, CD_3OD) δ: 0.83 (s, 9H), 1.96 (m, 2H), 2.20 (m, 2H), 2.28 (s, 3H), 2.46 (s, 3H), 2.62 (m, 1H), 2.68 (m, 1H), 2.81 (m, 1H), 2.88 (s, 3H), 2.92 (m, 1H), 4.33 (m, 3H), 4.90 (m,

2H), 6.45 (s, 1H), 7.15 (m, 9H). HRMS (ESI+): calculated for $C_{32}H_{41}N_5O_5$ [M + H] 576.3180; found 576.3185.

Benzyl(3*S*)-3-[(*tert*-butoxycarbonyl)amino]-4-[((1*S*)-1-{[(4-methylbenzyl)amino]carbonyl}-3-phenylpropyl)amino]-4-oxobutanoate (38)

2-Amino-*N*-(4-methylbenzyl)-4-phenylbutanamide hydrochloride (**5a**)[32] (1.5 g, 4.7 mmol) and *N*-(*tert*-butoxycarbonyl)-L-aspartic acid 4-benzyl ester (1.60 g, 4.94 mmol) in *N*,*N*-dimethylformamide (5.0 mL) was treated with HBTU (1.82 g, 4.80 mmol) and *N*-methylmorpholine (1.55 mL, 4.1 mmol) and stirred at ambient temperature for 16 h. The reaction mixture was poured into cold saturated $NaHCO_3$ solution and the precipitate collected, dried over $CaSO_4$ and subjected to chromatography on silica gel eluting with hexane–EtOAc gradient to give benzyl (3*S*)-3-[(*tert*-butoxycarbonyl)amino]-4-[((1*S*)-1-{[(4-methylbenzyl)amino]-carbonyl}-3-phenylpropyl)amino]-4-oxobutanoate **38** (2.5 g, 91%). ^{1}HMR (400 MHz, $CDCl_3$) δ: 1.44 (s, 9H), 1.98 (m, 1H), 2.28 (s, 3H), 2.65 (m, 2H), 2.75 (m, 1H), 2.87 (m, 1H), 4.35 (m, 1H), 4.37 (m, 1H), 4.47 (m, 2H), 5.00 (m, 2H), 5.52 (m, 1H), 6.86 (m, 1H), 7.00 (d, 1H), 7.12 (m, 8H), 7.30 (m, 7H).

32: ^{1}HMR (400 MHz, CD_3OD) δ: 0.83 (s, 9H), 2.51 (s, 3H), 2.73 (dd, $J = 12$ Hz, $J = 7$ Hz, 1H), 2.86 (dd, $J = 12$ Hz, $J = 7$ Hz, 1H), 2.90 (s, 2H) 2.95 (dd, $J = 12$ Hz, $J = 7$ Hz, 1H), 3.22 (dd, $J = 12$ Hz, $J = 7$ Hz, 1H), 4.48 (m, 2H), 4.66 (m, 1H), 6.46 (s, 1H), 7.15–7.25 (m, 7H), 7.39 (m, 1H).

tert-Butyl (*S*)-3-(3-*tert*-butyl-1,2,4-oxadiazol-5-yl)-1-((*S*)-1-(4-methylbenzylamino)-1-oxo-4-phenylbutan-2-ylamino)-1-oxopropan-2-ylcarbamate (40)

A solution of **38** (0.400 g, 0.681 mmol) in ethanol (50 mL) was treated with 10% palladium on carbon and subjected to hydrogenation under balloon pressure. After stirring at ambient temperature for 3 h the catalyst was removed by filtration and the solvent evaporated to give (3*S*)-3-[(*tert*-butoxycarbonyl)amino]-4-[((1*S*)-1-{[(4-methylbenzyl)amino]carbonyl}-3-phenylpropyl) amino]-4-oxobutanoic acid (**39**) (0.334 g, 98%) which was used without further purification. To a solution of compound **39** (0.225 g, 0.452 mmol) in dichloromethane (3.0 mL) and DMF (1.0 mL) was added *N*′-hydroxy-2,2-dimethylpropanimidamide (0.0625 g, 0.54 mmol) followed by *N*-(3-dimethylaminopropyl)-*N*′-ethylcarbodiimide hydrochloride (0.103 g, 0.54 mmol). The mixture was stirred for 16 hours and the dichloromethane evaporated under vacuo. The residue was treated with pyridine (3 mL) and heated under microwave irradiation at 110 °C for 20 min. The volatiles were evaporated and the residue subjected to preparative reverse phase HPLC on a C-18 column eluting with water–MeCN gradient to give **40** (150 mg, 57%). ^{1}H NMR (400 MHz, d_4-MeOH) δ: 1.32 (s, 9H), 1.41 (s, 9H), 1.97 (m, 1H), 2.10 (m, 1H), 2.29 (s, 3H), 2.62 (m, 2H), 3.30 (m, 2H), 4.33 (m, 3H), 4.63 (m, 1H), 7.13 (m, 7H), 7.22 (m, 2H).

N-((*S*)-3-(3-*tert*-Butyl-1,2,4-oxadiazol-5-yl)-1-((*S*)-1-(4-methylbenzylamino)-1-oxo-4-phenylbutan-2-ylamino)-1-oxopropan-2-yl)-5-methylisoxazole-3-carboxamide (37)

A solution of **40** (0.15 g, 0.26 mmol) in 1,4-dioxane (1 mL) was cooled in an ice bath and treated with a solution of 4 M HCl in dioxane (2.0 mL) and the mixture allowed to warm to ambient temperature. After stirring for 2 h, the solvent was evaporated and the residue treated with a solution of 5-methylisoxazole-3-carboxylic acid (0.036 g, 0.28 mmol), HBTU (0.148 g, 0.39 mmol) and *N*-methylmorpholine (57 μL, 0.5 mmol) in DMF (2.0 mL). The reaction mixture was stirred at ambient temperature for 4 h then diluted with water (100 mL) and extracted with dichloromethane. The extracts were dried ($MgSO_4$) and evaporated and the resulting crude product purified by reverse phase HPLC a on a C-18 column eluting with water–MeCN gradient to give *N*-((*S*)-3-(3-*tert*-butyl-1,2,4-oxadiazol-5-yl)-1-((*S*)-1-(4-methylbenzylamino)-1-oxo-4-phenylbutan-2-ylamino)-1-oxopropan-2-yl)-5-methylisoxazole-3-carboxamide (**37**) (70 mg, 46%). ^{1}H NMR (300 MHz, $CDCl_3$) δ: 1.32 (s, 9H), 1.95 (m, 1H), 2.15 (m, 1H), 2.31 (s, 3H), 2.47 (s, 3H), 2.58 (m, 2H), 3.15 (m, 1H), 3.50 (m, 1H), 4.34 (m, 3H), 5.08 (m, 1H), 6.24 (m, 1H), 6.40 (s, 1H), 7.10 (m, 5H), 7.21 (m, 5H), 8.25 (m, 1H). HRMS (ESI+): calculated for $C_{32}H_{38}N_6O_5$ [M + H] 587.2976; found 587.2982.

34: ^{1}HMR (400 MHz, CD_3OD) δ: 0.75 (t, $J = 8$ Hz, 3H), 1.33 (m, 2H), 1.85 (m, 2H), 2.10 (m, 2H), 2.21 (s, 3H), 2.39 (s, 3H), 2.53 (m, 1H), 2.63 (m, 1H), 2.76 (m, 1H), 2.92 (t, $J = 9$ Hz, 2H), 4.21 (m, 1H), 4.24 (s, 2H), 4.80 (m, 1H), 6.37 (s, 3H), 7.06 (m, 9H).

35: ^{1}HMR (400 MHz, CD_3OD) δ: 0.74 (d, $J = 8$ Hz, 6H), 1.58 (m, 1H), 1.85 (m, 2H), 2.10 (m, 2H), 2.20 (s, 3H), 2.38 (s, 3H), 2.70–2.48 (m, 3H), 2.78 (m, 2H), 4.21 (m, 1H), 4.24 (s, 2H), 4.80 (m, 1H), 6.37 (s, 3H), 7.06 (m, 9H).

High Resolution Mass Spectrometry (HRMS) data

Compound ***9***: HRMS (ESI+): calculated for $C_{36}H_{46}N_4O_4$ [M + H] 599.3597; found 599.3585.

Compound ***12***: HRMS (ESI+): calculated for $C_{29}H_{40}N_4O_4$ [M + H] 509.3122; found 509.3129.

Compound ***13***: HRMS (ESI+): calculated for $C_{32}H_{46}N_4O_4$ [M + H] 551.3592; found 551.3596.

Compound ***15***: HRMS (ESI+): calculated for $C_{35}H_{43}FN_4O_4$ [M + H] 603.3341; found 603.3347.

Compound ***16***: HRMS (ESI+): calculated for $C_{36}H_{46}N_4O_4$ [M + H] 599.3592; found 599.3597.

Compound ***17***: HRMS (ESI+): calculated for $C_{38}H_{50}N_4O_4$ [M + H] 627.3905; found 627.3908.

Compound ***19***: HRMS (ESI+): calculated for $C_{37}H_{43}N_5O_5$ [M + H] 638.3337; found 638.3343.

Compound ***20***: HRMS (ESI+): calculated for $C_{32}H_{41}N_5O_5$ [M + H] 576.3180; found 576.3185.

Compound ***21***: HRMS (ESI+): calculated for $C_{32}H_{44}N_4O_4$ [M + H] 549.3435; found 549.3430.

Compound ***22***: HRMS (ESI+): calculated for $C_{34}H_{40}ClFN_4O_4$ [M + H] 623.2795; found 623.2799.

Compound ***23***: HRMS (ESI+): calculated for $C_{35}H_{43}ClN_4O_4$ [M + H] 619.3046; found 619.3054.

Compound ***24***: HRMS (ESI+): calculated for $C_{40}H_{45}ClN_4O_5$ [M + H] 697.3151; found 697.3157.

Compound ***25***: HRMS (ESI+): calculated for $C_{36}H_{40}ClN_5O_5$ [M + H] 658.2791; found 658.2799.

Compound ***26***: HRMS (ESI+): calculated for $C_{31}H_{38}ClN_5O_5$ [M + H] 596.2640; found 596.2648.

Compound ***30***: HRMS (ESI+): calculated for $C_{29}H_{35}ClN_6O_5$ [M + H]; 583.2430; found 583.2432.

Compound ***31***: HRMS (ESI+): calculated for $C_{29}H_{35}ClN_6O_5$ [M + H] 583.2430; found 583.2434.

Compound ***32***: HRMS (ESI+): calculated for $C_{30}H_{35}Cl_2N_5O_5$ [M + H] 616.2093; found 616.2090.

Compound ***33***: HRMS (ESI+): calculated for $C_{24}H_{32}ClN_5O_5$ [M + H] 506.2165: found 506.2169.

Compound ***34***: HRMS (ESI+): calculated for $C_{30}H_{37}N_5O_5$ [M + H] 584.2873: found 584.2867.

Compound ***35***: HRMS (ESI+): calculated for $C_{31}H_{39}N_5O_5$ [M + H] 562.3029: found 562.3026.

Compound ***35***: HRMS (ESI+): calculated for $C_{31}H_{39}N_5O_5$ [M + H] 562.3029; found 562.3026.

Compound ***36***: HRMS (ESI+): calculated for $C_{37}H_{40}N_6O_5$ [M + H] 649.3133; found 649.3139.

Compound ***37***: HRMS (ESI+): calculated for $C_{32}H_{38}N_6O_5$ [M + H] 587.2976; found 587.2982.

We have reported the characterization of compounds **14**, **18**, **27**, **28**, **29** previously.[32]

Biological assays

NFκB reporter assay. Cells were seeded at 10 000 per well in white BioCoat™ poly-D-lysine (PDL)-coated 384-well plates (BD Biosciences) 16–24 h prior to compound treatment. HEK293 cells were pre-treated for 1 h with proteasome inhibitor and then stimulated with 10 ng mL^{-1} human recombinant tumor necrosis factor (rhTNF)-α (R&D Systems) for a further 3 h in the continued presence of the compound. Firefly luciferase activity was measured using Bright-Glo™ reagents according to the manufacturer's instructions (Promega) in a LEADseeker™ plate reader (GE Healthcare Life Sciences). Inhibition of NFκB-Luc activity was calculated relative to a no-compound (DMSO) control.

Cell viability assay. Calu6 cells (2000 cells per well) were plated in black/clear-bottom BioCoat™ poly-D-lysine (PDL)-coated 384-well plates (BD Biosciences) and were incubated with compound for 72 h, after which medium was removed to leave 25 μL per well. An equal volume of ATPlite™ reagent (PerkinElmer) was then added and luminescence was measured using a LEADseeker™ instrument.

Cell-based Proteasome-Glo β5 assays. Calu6 cells were plated as for the reporter assays and incubated with compound for 1 h at 37 °C. B-cell lymphoma subtypes Karpas-1106P, WSU-DLCL2 and OCI-Ly10 were plated at 20 000 cells per well in 384-well plates and treated with compounds identically. The activity of the 26S proteasome was measured *in situ* after compound removal by monitoring hydrolysis of the β5 (chymotrypsin-like) substrate Suc-LLVY-aminoluciferin (Promega) in the presence of luciferase using the Proteasome-Glo™ assay reagents according to the manufacturer's instructions (Promega). Luminescence was measured using a LEADseeker™ instrument.

In vitro **assays of purified 20S.** The peptidase activities of purified human erythrocyte and peripheral blood monocyte 20S proteasomes (Boston Biochem™) were assayed using fluorogenic tri- and tetra-peptide substrates coupled to 7-amino-4-methylcoumarin (AMC) (AnaSpec, Inc.) in the presence of recombinant proteasomal activator PA28α (Boston Biochem™). The following selective substrates were obtained from AnaSpec, Inc. with the exception of Z-LLE-AMC which was from Boston Biochem™ and were each used at a final concentration of 15 μM to assay the constitutive (c) and sub-sites: β1c, Z-LLE-AMC; β2c, Ac-KQL-AMC; β5c, Ac-WLA-AMC. Reactions were performed at 37 °C in 384-well black microtiter plates (Corning Inc.) using 0.25 nM 20S and 12 nM PA28α in a final volume of 50 μL buffer containing 20 mM HEPES, pH 7.4, 0.5 mM EDTA and 0.01% BSA. Peptidase activity was measured by monitoring AMC liberation over time with a Polarstar Galaxy fluorimeter (BMG Labtechnologies) using excitation and emission wavelengths of 340 nm and 460 nm, respectively. Percentage inhibition of 20S activity was calculated relative to the controls DMSO and 10 μM ML599698, an analog of bortezomib that contains a phenyl group in place of the *N*-terminal pyrazine cap.

X-ray crystallography. Crystals of purified wild-type and open-gated mutant 20S proteasome were grown in hanging drops at room temp, as described previously,[32] using a drop volume of 1.5 μL 20S (20 mg mL^{-1} in 10 mM Tris–HCl, pH 7.5, and 1 mM EDTA) and 0.5 μL of reservoir solution containing 100 mM MES, pH 7.0, 40 mM $Mg(CH_3COO)_2$, 15% 2-methyl-2,4-pentanediol (MPD), and 10 mM EDTA. Proteasome inhibitor complexes were generated by soaking crystals overnight in reservoir buffer containing 1 mM compound, 10% DMSO and 20% MPD followed by an additional 5 hours in reservoir buffer containing 1 mM compound, 10% DMSO and 25% MPD before being flash-cooled in liquid nitrogen. Crystal data and refinement statistics are given in the ESI Table†.

Acknowledgements

We are grateful to Juan Gutierrez and Zhi Li their assistance with preparation of the yeast 20S enzymes and to Abe Achab, David Lok, Nina Molchanova, Mingkun Fu and Ashok Patil for analytical chemistry assistance.

References

1 A. Hershko and A. Ciechanover, The ubiquitin system, *Annu. Rev. Biochem.*, 1998, **67**, 425–479.
2 A. L. Goldberg, Functions of the proteasome: from protein degradation and immune surveillance to cancer therapy, *Biochem. Soc. Trans.*, 2007, **35**, 12–17.
3 L. Borissenko and M. Groll, 20S Proteasome and its inhibitors, *Chem. Rev.*, 2007, **107**, 687–717.
4 J. Adams, V. J. Palombella, E. A. Sausville, J. Johnson, A. Destree, D. D. Lazarus, J. Maas, C. S. Pien, S. Prakash and P. J. Elliott, Proteasome inhibitors: a novel class of potent and effective antitumor agents, *Cancer Res.*, 1999, **59**, 2615–2622.
5 R. Z. Orlowski and D. J. Kuhn, Proteasome inhibitors in cancer therapy, *Clin. Cancer Res.*, 2008, **14**, 1649–1657.
6 J. Loewe, D. Stock, B. Jap, P. Zwickl, W. Baumeister and R. Huber, Crystal structure of the 20S proteasome from the archaeon T. acidophilin at 3.4.ANG resolution, *Science*, 1995, **268**, 533–539.
7 M. Groll, S. Ditzel, J. Lowe, D. Stock, M. Bochtler, H. D. Bartunik and R. Huber, Structure of the 20S proteasome from yeast at 2.4A.ANG. resolution, *Nature*, 1997, **386**, 463–471.
8 L. R. Dick and P. E. Fleming, Building on bortezomib: second-generation proteasome inhibitors as anti-cancer therapy, *Drug Discovery Today*, 2010, **15**, 243–249.
9 A. Baldisserotto, V. Ferretti, F. Destro, C. Franceschini, M. Marastoni, R. Gaviolo and R. Tomatis, α,β-Unsaturated *N*-acylpyrrole peptidyl derivatives: new proteasome inhibitors, *J. Med. Chem.*, 2010, **53**, 6511–6515.

10 D. J. Kuhn, R. Z. Orlowski and C. C. Bjorklund, Second generation proteasome inhibitors: carfilzomib and immunoproteasome-specific inhibitors, *Curr. Cancer Drug Targets*, 2011, **11**, 285–295.

11 P. P. Geurink, N. Liu, M. P. Spaans, S. L. Downey, A. M. C. H. van den Nieuwendijk, G. A. van der Marel, A. F. Kisselev, B. I. Florea and H. S. Overkleeft, Incorporation of fluorinated phenylalanine generates highly specific inhibitor of proteasome's chymotrypsin-like sites, *J. Med. Chem.*, 2010, **53**, 2319–2323.

12 R. M. Rydzewski, M. Burrill, R. Mendonca, J. T. Palmer, M. Rice, R. Tahilramani, K. E. Bass, L. Leung, E. Gjerstad, J. W. Janc and L. Pan, Optimization of sub-site binding to the β5 subunit of the human 20S proteasome using vinyl sulfones and 2-keto-1,3,4-oxadiazoles: syntheses and cellular properties of potent, selective proteasome inhibitors, *J. Med. Chem.*, 2006, **49**, 2953–2968.

13 R. H. Feling, G. O. Buchanan, T. J. Mincer, C. A. Kauffman, P. R. Jensen and W. Fenical, Salinosporamide A: a highly cytotoxic proteasome inhibitor from a novel microbial source, a marine bacterium of the new genus Salinospora, *Angew. Chem., Int. Ed.*, 2003, **42**, 355–357.

14 L. R. Reddy, J.-F. Fournier, B. V. S. Reddy and E. J. Corey, A new synthetic route for the enantioselective total synthesis of salinosporamide A and biologically active analogs, *Org. Lett.*, 2005, **7**, 2699–2701.

15 M. Groll, R. Huber and B. C. M. Potts, Crystal structures of salinosporamide A (NPI-0052) and B (NPI-0047) in complex with the 20S proteasome reveal important consequences of β lactone ring opening and a mechanism for irreversible binding, *J. Am. Chem. Soc.*, 2006, **128**, 5136–5141.

16 (*a*) P. C. Hogan and E. J. Corey, Proteasome inhibition by a totally synthetic β-lactam related to salinosporamide A and omuralide, *J. Am. Chem. Soc.*, 2005, **127**, 15386–15387; (*b*) P. Imbach, M. Lang, C. Garcıa-Echeverrıa, V. Guagnano, M. Noorani, J. Roesel, F. Bitsch, G. Rihs and P. Furet, Novel β-lactam derivatives: potent and selective inhibitors of the chymotrypsin-like activity of the human 20S proteasome, *Bioorg. Med. Chem. Lett.*, 2007, **17**, 358–362.

17 (*a*) J. Adams, M. Behnke, S. Chen, A. A. Cruickshank, L. R. Dick, L. Grenier, J. M. Klunder, Y.-T. Ma, L. Plamondon and R. L. Stein, Potent and selective inhibitors of the proteasome: dipeptidyl boronic acids, *Bioorg. Med. Chem. Lett.*, 1998, **8**, 333–338; (*b*) J. Adams, Development of the proteasome inhibitor PS-341, *Oncologist*, 2002, **7**, 9–16.

18 M. Groll, C. R. Berkers, H. L. Ploegh, H. Ovaa, M. Groll, C. R. Berkers, H. L. Ploegh and H. Ovaa, Crystal structure of the boronic acid-based proteasome inhibitor bortezomib in complex with the yeast 20S proteasome, *Structure*, 2006, **14**, 451–456.

19 E. Kupperman, E. C. Lee, Y. Cao, B. Bannerman, M. Fitzgerald, A. Berger, J. Yu, Y. Yu, F. Bruzzese, J. Liu, J. Blank, K. Garica, C. Tsu, L. Dick, P. Fleming, L. Yu, M. Manfredi, M. Rolfe and J. Bolen, Evaluation of the proteasome inhibitor MLN9708 in preclinical models of human cancer, *Cancer Res.*, 2010, **70**, 1970–1980.

20 B. D. Dorsey, M. Iqbal, S. Chetterjee, E. Menta, R. Bernadini, A. Bernareggi, P. G. Cassara, G. D'Arasmo, E. Ferretti, S. De Munari, A. Oliva, G. Pezzoni, C. Allievi, I. Strepponi, B. Ruggeri, M. A. Ator, M. Williams and J. P. Mallamo, Discovery of a potent, selective and orally active proteasome inhibitor for the treatment of cancer, *J. Med. Chem.*, 2008, **51**, 1068–1072.

21 E. Sanchez, L. Mingjie, J. A. Steinberg, C. Wang, J. Shen, B. Bonavida, Z. Li, H. Chen and J. R. Berenson, The proteasome inhibitor CEP-18770 enhances the anti-myeloma activity of bortezomib and melphalon, *Br. J. Haematol.*, 2010, **148**, 569–581.

22 (*a*) O. A. O'Connor and M. S. Czuczman, Novel approaches for the treatment of NHL: proteasome inhibition and immune modulation, *Leuk. Lymphoma*, 2008, **49**(suppl. 1), 59–66; (*b*) P. G. Richardson, E. Weller, S. Lonial, A. J. Jakubowiak, S. Jagannath, N. S. Raje, D. E. Avigan, W. Xie, I. M. Ghobrial, R. L. Schlossman, A. Maxumder, N. C. Munchi, D. H. Vesole, R. Jotce, J. L. Kaufman, D. Doss, D. L. Warren, L. E. Lunde, S. Kastrer, C. DeLanay, T. Hideshima, C. S. Mitsiades, R. Knight, D. L. Esseltine and K. C. Anderson, Lenalidomide, bortezomib, and dexamethasone combination therapy in patients with newly diagnosed multiple myeloma, *Blood*, 2010, **116**, 679–686.

23 (*a*) Y. Koguchi, J. Kohno, M. Nishio, K. Takahashi, T. Okuda, T. Ohnuki and S. Komatsubara, TMC 95 A, B, C and D, novel proteasome inhibitors produced by *Apiospora montagnei* Sacc. TC-1093. Taxonomy, production, isolation, and biological activities, *J. Antibiot.*, 2000, **53**, 105–109; (*b*) M. Groll, Y. Koguchi, R. Huber and J. Kohno, Crystal structure of the 20S proteasome:TMC-95A complex: a non-covalent proteasome inhibitor, *J. Mol. Biol.*, 2002, **311**, 543–548.

24 M. Groll, M. Gotz, M. Kaiser, E. Weyher and L. Moroder, TMC-95-based inhibitor design provides evidence for the catalytic versatility of the proteasome, *Chem. Biol.*, 2006, **13**, 607–614.

25 N. Basse, S. Piguek, D. Papapostolou, A. Ferrier-Berthelot, N. Richey, M. Pagano, P. Sarthou, J. Sobczak-Thepot, M. Reboud-Ravaux and J. Vidal, Linear TMC-95-based proteasome iinhibitors, *J. Med. Chem.*, 2007, **50**, 2842–2850.

26 C. García-Echeverría, P. Imbach, D. France, P. Furst, M. Lang, M. Noorani, D. Scholz, J. Zimmermann and P. Furet, A new structural class of selective and non-covalent inhibitors of the chymotrypsin-like activity of the 20S proteasome, *Bioorg. Med. Chem. Lett.*, 2001, **11**, 1317–1319.

27 P. Furet, P. Imbach, P. Furst, M. Lang, M. Noorani, J. Zimmermann and C. Garcia-Echeverria, Modeling of the binding mode of a non-covalent inhibitor of the 20S proteasome. Application to structure-based analog design, *Bioorg. Med. Chem. Lett.*, 2001, **11**, 1321–1324.

28 P. Furet, P. Imbach, P. Furst, M. Lang, M. Noorani, J. Zimmermann and C. Garcia-Echeverria, Structure-based optimization of 2-aminobenzylstatin derivatives: potent and selective inhibitors of the chymotrypsin-like activity of the human 20S proteasome, *Bioorg. Med. Chem. Lett.*, 2002, **12**, 1331–1334.

29 P. Furet, P. Imbach, M. Noorani, J. Koeppler, K. Laumen, M. Lang, V. Guagnano, P. Fuerst, J. Roesel and C. Garcia-Echeverria, Entry into a new class of potent proteasome inhibitors having high anti-proliferative activity by structure-based design, *J. Med. Chem.*, 2004, **47**, 4810–4813.

30 R. T. Lum, S. S. Kerwar, S. M. Meyer, M. G. Nelson, S. R. Schow, D. Shiffman, M. M. Wick and A. Joy, A new structural class of proteasome inhibitors that prevent NF-kappa B activation, *Biochem. Pharmacol.*, 1998, **55**, 1391–1397.

31 R. T. Lum, M. G. Nelson, A. Joly, A. G. Horsma, G. Lee, S. M. Meyer, M. M. Wick and S. R. Schow, Selective inhibition of the chymotrypsin-like activity of the 20S proteasome by 5-methoxy-1-indanone dipeptide benzamides, *Bioorg. Med. Chem. Lett.*, 1998, **8**, 209–214.

32 C. Blackburn, K. Gigstad, P. Hales, K. Garcia, M. Jones, F. Bruzzese, C. Barrett, J. Liu, T. Soucy, D. Sappal, N. Bump, E. Olhava, P. Fleming, L. R. Dick, C. Tsu, M. Sintchak and J. L. Blank, Characterization of a new series of non-covalent proteasome inhibitors with exquisite potency and selectivity for the 20S β5-subunit, *Biochem. J.*, 2010, **430**, 461–476.

33 C. Blackburn, F. Bruzzese, C. Barrett, J. Blank, N. Bump, M. Jones, C. Tsu, P. Fleming, M. Sintchak, P. Hales, D. Sappal, L. Dick, K. Garcia, K. Gigstad, L. Herman and J. Liu, Optimization of the β5 Potency and Cellular Activity of a Series of Non-covalent Dipeptide Inhibitors of the Human 20S Proteasome Guided by X-Ray Crystallography, *Abstracts, 37th Northeast Regional Meeting of the American Chemical Society*, Potsdam, NY, US, June 2–5 (2010), NERM-198.

34 C. Blackburn, C. Barrett, J. L. Blank, F. Bruzzese, N. Bump, L. R. Dick, P. Fleming, K. Garcia, P. Hales, M. Jones, J. X. Liu, D. S. Sappal, M. D. Sintchak, C. Tsu and K. M. Gigstad, Optimization of a series of dipeptides with a P3 threonine residue as non-covalent inhibitors of the chymotrypsin-like activity of the human 20S proteasome, *Bioorg. Med. Chem. Lett.*, 2010, **20**, 6581–6586.

35 C. Blackburn, J. Blank, N. Bump, F. Bruzzese, L. Dick, P. Fleming, K. Garcia, K. Gigstad, P. Hales, L. Herman, M. Jones, Z. Li, J. X. Liu, A. Mishechkina, M. Nagayoshi, D. Sappal, M. Sintchak and C. Tsu, Series of Non-covalent Inhibitors of the 20S Proteasome Derived from *N*-β-neopentyl Asparagine with Unprecedented Potency and Selectivity, *Abstracts of Papers, 240th National ACS meeting*, Boston, MA, August 22–26, (2010), MEDI-235.

36 S. Borg, G. Estenne-Bouhtou, K. Luthman, I. Csoregh, W. Hesselink and U. Hacksell, Synthesis of 1,2,4-oxadiazole-, 1,3,4-oxadiazole-, and 1,2,4-triazole-derived dipeptidomimetics, *J. Org. Chem.*, 1995, **60**, 3112–3120.

37 Proteasomal degradation of the inhibitory protein IκBα, (following its phosphorylation and ubiquitination) activates the NFκB transcription factor in cells in response to TNFα stimulation.[30] See also: V. J. Palombella, O. J. Rando, A. L. Goldberg and T. Maniatis, The ubiquitin proteasome pathway is required for processing the NF-κB1 precursor protein and the activation of NF-κB, *Cell*, 1994, **78**, 773–785.